Inhibition of Thiol-Mediated Uptake with Irreversible Covalent Inhibitors

Lim, Bumhee; Cheng, Yangyang; Kato, Takehiro; Pham, Anh Tuan; Le Du, Eliott; Mishra, Abhaya Kumar; Grinhagena, Elija; Moreau, Dimitri; Sakai, Naomi; Waser, Jérôme; Matile, Stefan

How to cite

LIM, Bumhee et al. Inhibition of Thiol-Mediated Uptake with Irreversible Covalent Inhibitors. In: Helvetica Chimica Acta, 2021, vol. 104, n° e2100085, p. 1–9. doi: 10.1002/hlca.202100085

This publication URL: https://archive-ouverte.unige.ch/unige:153636
Publication DOI: 10.1002/hlca.202100085

doi.org/10.1002/hlca.202100085

COMMUNICATION

HELVETICA chimica acta

Inhibition of Thiol-Mediated Uptake with Irreversible Covalent Inhibitors

Bumhee Lim[+,a,b] Yangyang Cheng[+,a,b] Takehiro Kato[+,a,b] Anh-Tuan Pham,[a,b] Eliott Le Du,[c] Abhaya Kumar Mishra,[b,c] Elija Grinhagena,[b,c] Dimitri Moreau,[b] Naomi Sakai,[a,b] Jerome Waser,*[b,c] and Stefan Matile*[a,b]

[a] Department of Organic Chemistry, University of Geneva, Quai Ernest Ansermet 30, CH-1211 Geneva 4, Switzerland, e-mail: stefan.matile@unige.ch

[b] National Centre of Competence in Research (NCCR) Chemical Biology, Quai Ernest Ansermet 30, CH-1211 Geneva 4, Switzerland

[c] Laboratory of Catalysis and Organic Synthesis, Ecole Polytechnique Fédérale de Lausanne EPFL SB ISIC LCSO, BCH 4306, 1015 Lausanne, Switzerland, e-mail: jerome.waser@epfl.ch

Dedicated to *Peter Kündig* on the occasion of his 75th birthday

Thiol-mediated uptake is emerging as method of choice to penetrate cells. This study focuses on irreversible covalent inhibitors of thiol-mediated uptake. High-content high-throughput screening of the so far largest collection of hypervalent iodine reagents affords inhibitors that are more than 250 times more active than *Ellman*'s reagent and rival the best dynamic covalent inhibitors. Comparison with other irreversible reagents reveals that inhibition within one series follows reactivity, whereas inhibition across series deviates from reactivity. These trends support that molecular recognition, besides dynamic covalent exchange, contributes significantly to thiol-mediated uptake. The most powerful inhibitors besides the best hypervalent iodine reagents were *Fukuyama*'s nosyl protecting group and super-cinnamaldehydes that have been introduced as irreversible activators of the pain receptor TRPA1. Considering that several viruses use different forms of thiol-mediated uptake to enter cells, the identification of new irreversible inhibitors of thiol-mediated uptake is of general interest for the discovery of new antivirals.

Keywords: antiviral agents, hypervalent compounds, hypervalent iodine reagents, inhibitors, nosyl protecting group, thiol-mediated uptake, TRPA1 pain receptor.

Thiol-mediated uptake is an intriguing process because it works so well but is so poorly understood.[1] The ability of oligochalcogenides, usually disulfides, to facilitate cell penetration has been observed in many variations.[2–14] The unifying theme is dynamic covalent oligochalcogenide exchange with thiols (and/or disulfides) on the cell surface that can be inhibited by thiol reactive agents (*Figure 1,a*). This central dynamic covalent chemistry process can be coupled to diverse uptake mechanisms, including endocytosis, fusion and also direct translocation across the plasma membrane directly into the cytosol.

Early examples on thiol-mediated uptake focus mainly on the entry of viruses into cells. Particular emphasis has been on HIV, which proceeds by fusion after the essential dynamic-covalent exchange with protein disulfide isomerases on cell surfaces.[15] More recently, privileged scaffolds such as CPDs (cell-penetrating poly(disulfide)s) and COCs (cyclic oligochalcogenides)[16] have been introduced to exploit thiol-mediated uptake for the efficient delivery of

[+] These authors contributed equally to this study.

Supporting information for this article is available on the WWW under https://doi.org/10.1002/hlca.202100085

a broad variety of substrates into the cytosol.[1] This includes substrates that are significant and, depending on the context, often problematic to deliver otherwise, *e.g.*, antibodies,[4] DNA/RNA, nanoparticles,[7] artificial enzymes,[17] quantum dots,[18] liposomes and polymersomes.[19]

Ellman's reagent has been the benchmark inhibitor to probe for thiol-mediated uptake until recently.[20] This choice has not been beneficial for the field, because 5,5′-dithio-bis(2-nitrobenzoic acid) (DTNB) is a notoriously weak and unreliable inhibitor. The poor performance of *Ellman*'s reagent is reasonable considering that it produces activated disulfides on cell surfaces that readily continue to exchange. Together with challenges in target identification with dynamic networks,[1] unreliable DTNB data have helped to raise questions concerning significance, nature and even the very existence of thiol-mediated uptake. Earlier this year, these overall unnecessary questions have been addressed with a broad inhibitor screening.[20] Up to 5000 times more powerful inhibitors were found. In preliminary tests, a few of the identified inhibitors also inhibited the entry of SARS-CoV-2 spike pseudo-lentiviruses, with efficiencies clearly exceeding the popular ebselen[21,22] (mostly unpublished). It remains to be seen whether or not this is more than a coincidence. The same holds for the transferrin receptor (among many other possible targets), found in both proteomics screens for thiol-mediated uptake of COCs[23] as well as contributing to the entry of SARS-CoV-2.[24]

Inhibitor screening for thiol-mediated uptake has so far focused on dynamic covalent inhibitors.[20] The objective of this study was to shift attention to irreversible inhibition. Particular emphasis is on hypervalent iodine reagents of different structure and reactivity (*Figure 1,b*). Hypervalent iodine reagents centered around the ethynyl benziodoxolone (EBX) scaffold react with high rate with thiols.[25,26] They have been used previously in proteomics studies of the cysteinome, and excelled with unique reactivity and selectivity.[27] Other applications include further derivatizations of cysteines,[28,29] peptide Cys-Cys and Cys-Lys stapling,[30] functional terminators of CPDs,[31] and classical use as alkynylation reagents in organic synthesis.[32,33] The results from irreversible inhibition of thiol-mediated uptake with hypervalent iodine reagents are then compared to classical and modern irreversible thiol-reactive agents.[34–45] Hypervalent iodine reagents emerge top, together with *Fukuyama*'s nosyl protecting group[34] and super-cinnamaldehyde

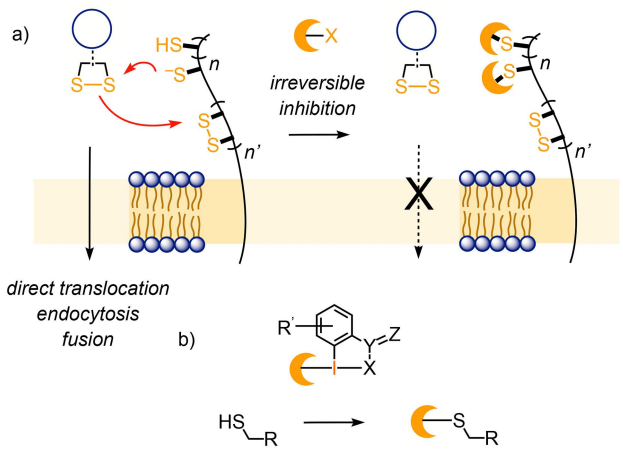

Figure 1. a) Thiol-mediated uptake operates with inhibitable dynamic covalent chalcogen exchange cascades before or during cellular entry by direct translocation, endocytosis or fusion, usually thiol/disulfide exchange. b) General scheme for inhibition with irreversible covalent inhibitors.

ligands of the pain receptor TRPA1,[35] all rivaling the best reversible inhibitors.

The inhibitor candidates **1**–**25** tested in this study were numbered to roughly reflect their identified activity, decreasing with increasing numbers, with DTNB ending up as number **25** (*Figure 2*). They were synthesized mostly following reported procedures (see *Supporting Information*).

For inhibitor screening of thiol-mediated uptake, the conjugate **26** composed of an epidithiodiketopiperazine (ETP), *i.e.*, one of the most active COCs,[46] and fluorescein (FITC) was used as reporter (*Figure 3*). FITC-ETP **26** rapidly penetrates unmodified HeLa cells to end up staining cytosol and nucleus.[46] In this assay, inhibition of thiol-mediated uptake is detected as decreasing fluorescence of the cells (*Figure 3*). For inhibitor screening, a recently introduced fully automated, fluorescent microscopy image-based high-content high-throughput screening (HCHTS) was used.[20,47] Namely, HeLa cells in multiwell plates were incubated first with inhibitor candidates for a given period of time. Then, reporter **26** was added to penetrate cells within 30 minutes. Afterward, the multiwell plates were washed to remove all reporter and inhibitor candidates in the media, *Hoechst 33342* and propidium iodide were added for automated analysis, and the CSLM images were recorded. *Hoechst 33342* is a cell-permeable DNA stain applied to stain all cells, propidium iodide is a cell-impermeable DNA stain used to differentiate necrotic and apoptotic from healthy cells. Relative cell viability (*RV*) was calculated

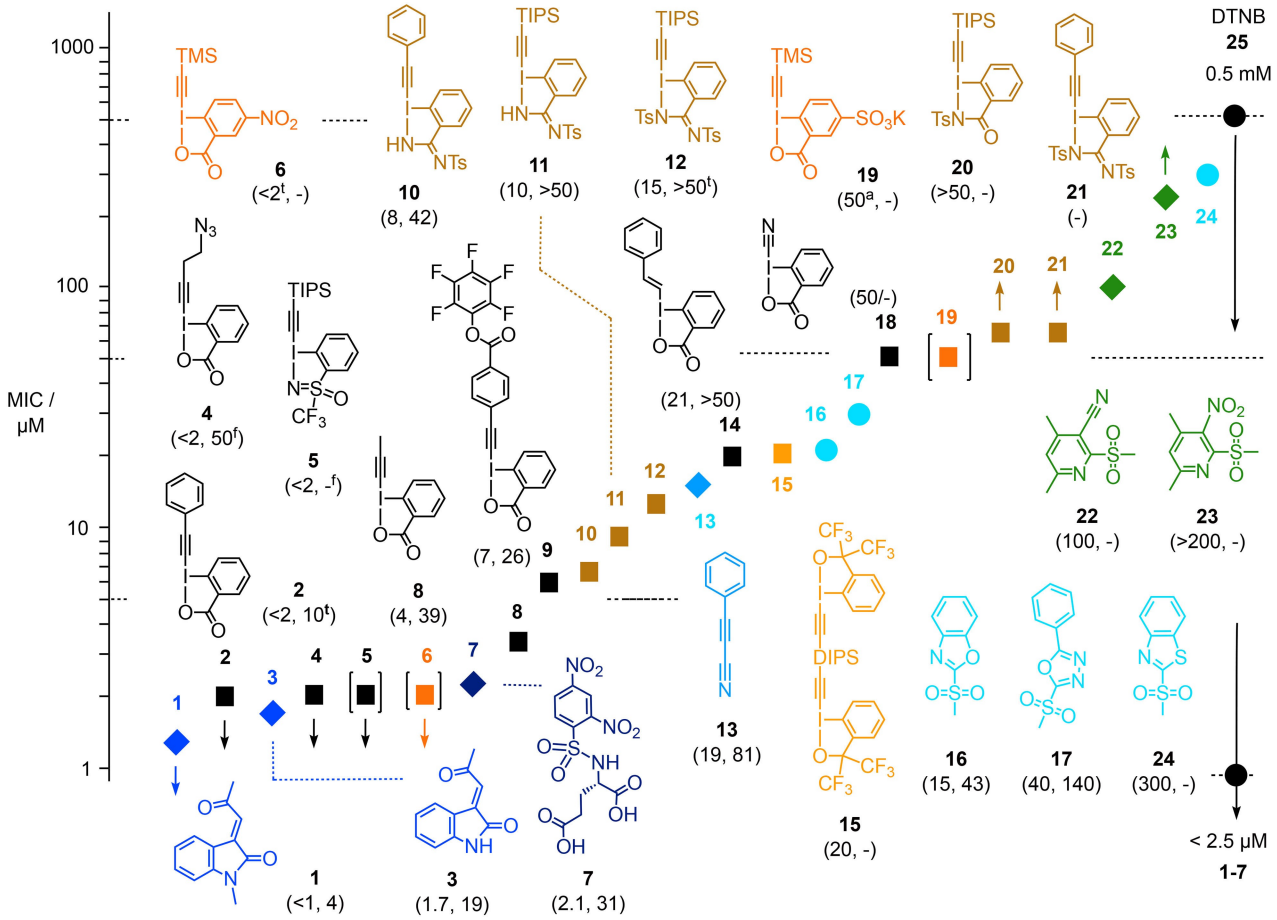

Figure 2. Structure of inhibitor candidates **1**–**24** with their concentrations needed to inhibit by *ca.* 15% (MIC) the thiol-mediated uptake of fluorescently-labeled ETP **26**. All results were obtained by 1 h pre-incubation of HeLa cells with inhibitor candidates, followed by 30 min incubation with reporter **26**. Below compound numbers are given, in parenthesis, first MIC, then, if detectable, IC_{50}, both in µM. t, onset of toxicity; f, 'flat' dose-response curve (see text); a, onset of activation of uptake; upward arrows, MIC not reached at indicated concentration; downward arrows, MIC already passed at indicated concentration (compare dose response curves, *Figures 4*, *S1*–*S4*). MIC values indicated by symbols in brackets are approximate.

automatically from the ratio of propidium iodide and *Hoechst 33342* labeled cells (*Figure 4*; results were backed up with MTT cell viability assays for selected inhibitors, *Figure S5*). Propidium iodide negative cells were kept to determine average fluorescence intensity from reporter **26** for intact cells only. This fully automated procedure was important to secure quantitative data on both uptake and toxicity, and to record uptake independent from toxicity. In other words, uptake data refer to intact cells exclusively, even at high toxicity.

In this assay, it is possible to remove inhibitor candidates from the media before reporter addition, a method referred to as 'pre-incubation' which, in principle, excludes direct interaction between reporter and inhibitor and thus limits inhibitor exchange to cellular target. The alternative addition of reporter without prior inhibitor removal is referred to as 'co-incubation' method, which, in principle, does not exclude direct interaction between reporter and inhibitors that have not reacted before with cellular targets.

The results of HCHT inhibitor screening were ranked according to their MIC, that is the minimal inhibitory concentration needed to inhibit the thiol-mediated uptake of FITC-ETP **26** by *ca.* 15% (*Figure 2*). MICs were preferable over IC_{50}'s, that is the concentration needed for 50% inhibition, because competing high concentration effects such as toxicity, precipitation or even activation, could produce highly unusual dose response curves (*Figure 4*). Such anomalous concentration dependence is also the origin of conflicting results with *Ellman*'s reagent **25**, which reaches MIC around 0.5 mM and loses this marginal activity

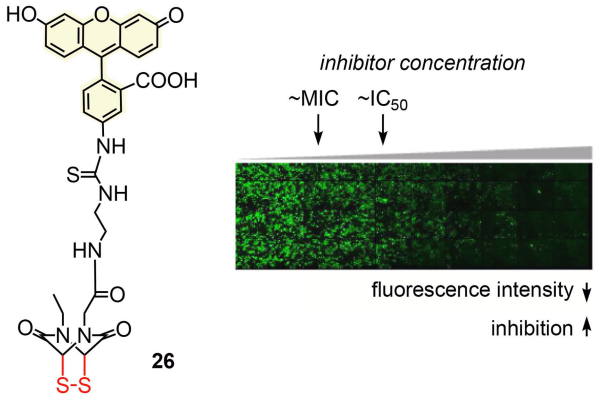

Figure 3. Structure of FITC-ETP reporter **26** and representative multiwell plate for automated HCHT inhibitor screening of HeLa Kyoto cells incubated first with, from left to right, increasing concentrations of an inhibitor and then with a constant concentration of **26**. Each green dot represents at least one HeLa cell penetrated by **26**, and the response in decreasing fluorescence of cells to increasing concentration characterizes the efficiency of the inhibitor, quantified in MIC and IC_{50}, see *Figure 2*.

again at higher concentrations due to the onset of weak uptake activation (*Figure 2*). Such uptake activation at high concentrations often indicates the onset of membrane damage and coincides with the onset of cytotoxicity (*Figures 4,i* and *4,j*).

The ability of hypervalent iodine reagents to inhibit thiol-mediated uptake varied enormously, covering the full range of MICs <2 μM to undetectable inhibition at >100 μM (*Figure 2*). In general, increasing inhibition activity coincided beautifully with increasing reactivity of the hypervalent iodine reagent. The most impressive MICs were obtained for the classical ethynyl benziodoxolone such as **2**, **4**, **6**, **8** and **9**.[26,27,29,30] Substitution of the terminal phenyl in ethynyl benziodoxolone **2** with a methyl in **8** reduced activity to MIC = 4 μM but improved dose response curve profiles with regard to toxicity at higher concentration (*Figures 2*, *4,a* and *4,e*).

Replacement of the benziodoxolone in **2** with a less reactive, *N*-stabilized benziodazolimine in **10**[48] caused the respective drop from MIC <2 μM to MIC = 8 μM, together with an attractive decrease in toxicity at higher concentrations (*Figures 2*, *4,b* and *4,e*). Tosylation of the second nitrogen in benziodazolimine **10** gave the completely inactive **21** with an MIC >100 μM (*Figures 2*, *4,b* and *4,c*).[48] This inactivation by tosylation was again consistent with the poor reactivity of **21**, which is caused by a halogen bond[49–52] from the tosyl oxygen acceptor to the hypervalent iodine donor (*Figure 5*).[48] Similar inactivation by intramolecular σ-hole interactions has already been observed for anion transport with chalcogen bonds[53] as well as catalysis with pnictogen bonds,[54] and used extensively in the design of fluorescent flipper probes.[53,55] Replacement of the terminal phenyl group with a TIPS gave the same trend with **11** and **12**, although clearly less pronounced (*Figure 2*). Benziodazolone **20** was inactive, whereas increasing reactivity with an activated benziodosulfoximine **5** afforded the expected low MIC <2 μM together with, however, an inacceptable dose response curve (*Figures 2*, *4,h*; *vide infra*).

Replacement of the alkyne in benziodoxolone **2** with an alkene in vinylbenziodoxolone[56] **14** reduced activity as expected from reduced reactivity (*Figures 2*, *4,d* and *4,e*). Similarly reduced activity of the highly reactive nitrile **18** is presumably due to instability in water. Activation of the benziodoxolone in **2** with a nitro acceptor in *para* position gave **6** with an excellent MIC <2 μM together with excessive toxicity (*Figures 2*, *4,e* and *4,g*). The anionic sulfonate acceptor in the analogous **19**[57] resulted in uptake activation rather than inhibition above 50 μM (*Figure 2*). Such activation often coincides with the onset of toxicity and has been attributed to membrane-disrupting detergent-like activity at higher concentration. This interpretation was in good agreement with the amphiphilic structure of the anion **19**.

The ethynyl benziodoxole dimer **15**, originally conceived for peptide stapling,[30] was attractive with regard to the recognition of neighboring thiols on the cell surface. However, the modest performance with MIC = 20 μM was dominated by the reduced reactivity rather than divalency (*Figure 2*). The same was true for **9** with MIC = 8 μM, which was designed for Cys-Lys stapling in aprotic media,[30] but presumably hydrolyzed to the carboxylate before reacting at the cell surface (*Figure 2*).

The most active hypervalent iodine reagents with MIC ≤ 2 μM showed less than perfect dose response curves. Ethynyl benziodoxolone **2** suffered from a rather early onset of toxicity, exceeding activity above the IC_{50} = 10 μM (*Figure 4,e*). Azide **4** showed an intriguing, almost concentration independent inhibition around 30% from MIC ≤ 2 μM until the onset of toxicity >50 μM (*Figure 4,f*). As already mentioned, competing precipitation or the onset of toxicity related activation could contribute to this apparent concentration independence. Moreover, the environment-dependent contributions from the addition of exofacial thiols **27** to yield alkene **28** rather than the standard substitution product **29** could contribute to unusual dose response (*Figure 5*).[28] The same behav-

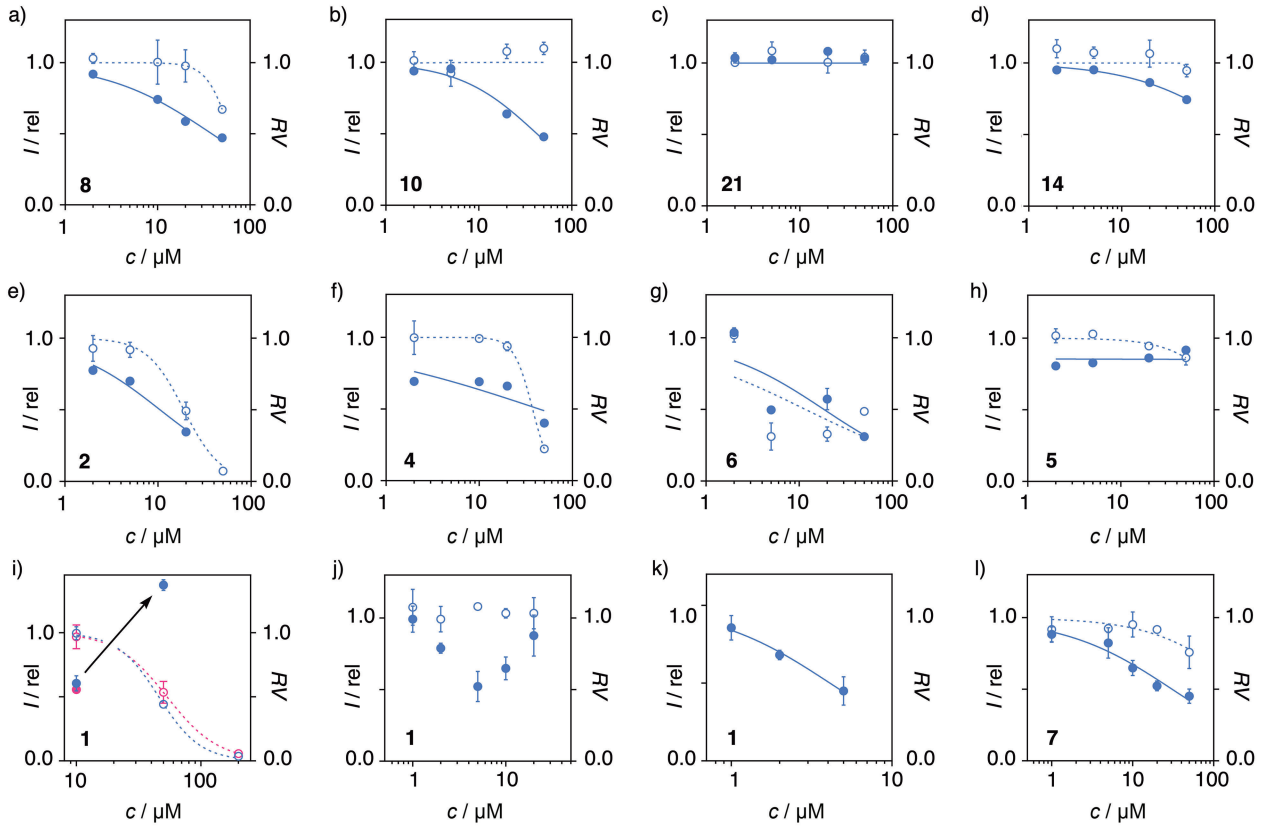

Figure 4. Representative HCHTS profiles showing relative fluorescence intensity *I* (filled symbols) and relative cell viability *RV* (empty symbols) of HeLa Kyoto cells after incubation with a) **8**, b) **10**, c) **21**, d) **14**, e) **2**, f) **4**, g) **6**, h) **5**, i–k) **1** and l) **7** for 1 h at the indicated concentrations, followed by incubation with the fluorescent reporter **26** (10 µM) for 30 min. i–k) Screening optimization for **1**: i) Initial tests revealing the onset of toxicity (empty symbols) and toxicity related activation (arrow) between 10 and 50 µM; blue: 1 h, pink: 30 min incubation with **26**; j) focused tests at lower concentrations, demonstrating the onset of toxicity related activation between 5 and 10 µM; k) curve fit for inhibition until onset of activation above 5 µM, revealing MIC and IC_{50}.

ior at weaker inhibition of *ca.* 15% was observed with **5** (*Figure 4,h*), while **6** was simply too toxic to be considered (*Figure 4,g*). More convincing dose response curves appeared with **8** at MIC = 4 µM (*Figure 4,a*). The less reactive amidines generally excelled with low toxicity also at high concentrations. The dose response curves for **10** with an MIC = 8 µM could be completed below a high IC_{50} = 42 µM without the appearance of toxicity (*Figure 4,b*).

Irreversible inhibition of thiol-mediated uptake with hypervalent iodine reagents compared favorably to other reagents. Tunable heteroaromatic sulfones like **16** have been introduced recently as bioorthogonal probes for cysteine profiling.[37] They react with thiols by nucleophilic aromatic substitution, affording aryl sulfides **30** (*Figure 5*). As reported previously,[20] inhibition of thiol-mediated uptake with heteroaromatic sulfones nicely follows reactivity from **24** with MIC = 300 µM over **17** with MIC = 40 µM to **16** with MIC = 15 µM, but overall activities were not competitive (*Figure 2*). The same was true for the related, electron-deficient 2-sulfonylpyridines **22** and **23** introduced by *Zambaldo et al.* for the targeted labeling of proteins with stable aryl sulfides **31** (*Figure 5*).[38] Activities increased from **23** to **22**, but the best MIC = 100 µM was not impressive, only five times better than *Ellman*'s reagent (*Figure 2*).

The 3-arylpropiolonitrile **13** introduced by *Wagner* and coworkers[36] for ultrafast, bioorthogonal and irreversible conjugate 'click' addition of cysteines to afford conjugates **32** gave better results, with an MIC = 19 µM and an onset of competing activation visible above 50 µM (*Figures 2* and *5*). The most positive surprise, however, was DNs protected glutamate **7**. A classic in organic synthesis, nosyl deprotection occurs also by nucleophilic aromatic substitution with thiols **27** to afford sulfide **33** besides the deprotected amine and SO_2 (*Figure 5*).[34] Inhibition of thiol-mediated

uptake of reporter **26** by DNs **7** occurred with an MIC = 2.1 μM, an IC_{50} = 31 μM and a dose response curve without significant anomalies (*Figures 2* and *4,l*).

Among the best inhibitors were super-cinnamaldehydes **1** and **3**. These activated *Michael* acceptors were introduced by *Cravatt*, *Schultz* and coworkers to elucidate the mode of action of TRPA1 (transient receptor potential ankyrin 1).[35] TRPA1 is an ion channel that is activated by pain, cold and itch, responding to noxious stimuli from pungent natural products such as cinnamaldehyde, mustard oil, or allicin from garlic.[35,58] Super-cinnamaldehydes **1** and **3** were rationally designed to explore whether or not the ion channel is activated by conjugate addition of thiols. Their activity was found to exceed cinnamaldehyde, thus validating the hypothesis of covalent ion channel activation. Conjugate addition to yield sulfide **34** was shown to be irreversible (*Figure 5*).[35] Molecular recognition by TRPA1 is likely to direct the regioselectivity of the *Michael* addition to mimic cinnamaldehyde as drawn in **34**, whereas intrinsic reactivity in solution should favor addition to the exocyclic carbon.[59]

The inhibition of thiol-mediated uptake of reporter **26** by super-cinnamaldehydes was slightly better for the more hydrophobic **1** than for **3** (*Figure 2*). Both *Michael* acceptors gave anomalous dose response curves in initial screens, with promising inhibition around 10 μM changing to significant activation and high toxicity at 50 μM (*Figure 4,i*). Focused screening around 10 μM gave a sub-micromolar MIC < 1 μM and a minimum around the IC_{50} = 4 μM, followed by decreasing inhibition at higher concentrations due to increasingly dominant uptake activation (*Figure 4,j*). Remarkably, this IC_{50} = 4 μM of super-cinnamaldehyde **1** was below the best hypervalent iodine reagent **2** with IC_{50} = 10 μM and not affected by cytotoxicity at this relevant concentration (*Figures 2* and *4,i*).

It would be premature to conclude that TRPA1 can contribute to thiol-mediated uptake. The cysteines

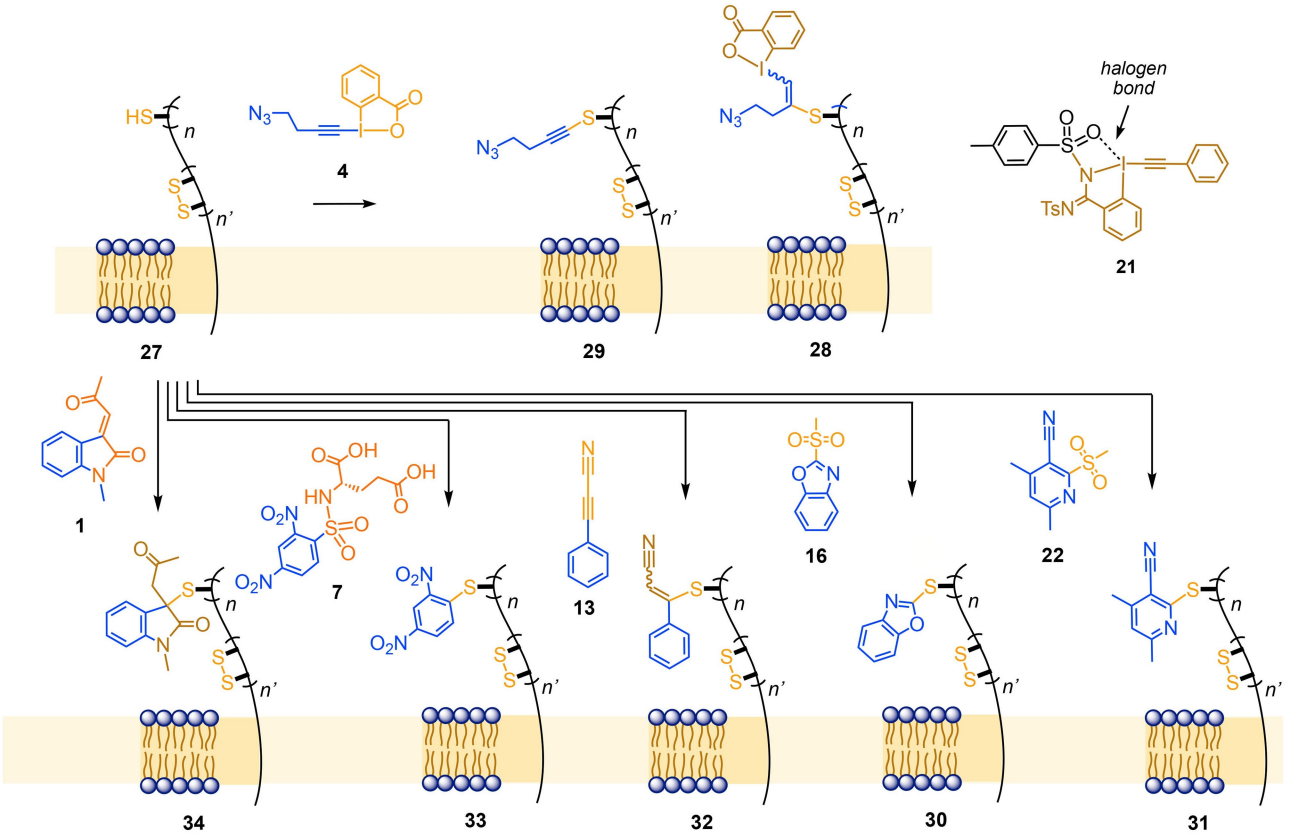

Figure 5. Irreversible reactions of hypervalent iodine reagents compared to other key motifs with thiols on cell surfaces. Substitution products like **29** are generally preferred, addition products like **28** occur with alkyl alkynes, depending on the environment. An intramolecular halogen bond is thought to account for reduced reactivity of **21** and related inhibitors.

targeted by super-cinnamaldehyde **1** are on the luminal side of the ion channel and not accessible by larger substrates. However, TRPA1 contains cysteines within transmembrane helices that could conceivably be involved in thiol-mediated uptake as outlined elsewhere.[1] More likely, however, is that super-cinnamaldehydes **1** and **3** react with other, so far unknown targets on the cell surface with exofacial thiols that mediate cellular uptake.

In summary, screening of the so far largest collection of hypervalent iodine reagents to inhibit thiol-mediated uptake of a fluorescent ETP reporter afforded activities that, with MIC < 2 μM, rival the best COCs identified so far and exceed the activity of the benchmark DTNB more than 250 times. Inhibition overall correlated well with reactivity. Anomalous dose response curves could be rationalized with the onset of activation by membrane destabilization and, perhaps, aggregation and precipitation. Activities compare well with other irreversible thiol-reactive agents, which increase with reactivity within a given class but vary strongly between different classes. These reactivity-independent variations demonstrate that thiol-mediated uptake operates with important selectivity, that is molecular recognition. Similarly significant contributions from molecular recognition have been observed in proteomics studies with the same and similar thiol-reactive probes. Each probe labeled different protein families in the cysteinome.[27,37,44] Thiol-mediated uptake thus emerges as functional system to elucidate parts of the cysteinome 'in action'.

The distinct signatures of irreversible inhibitors further confirm that thiol-mediated uptake exists and involves significant molecular recognition. Simple passive diffusion also of small-molecule reporters like **26** across the plasma membrane can thus be excluded. Together with hypervalent iodine reagents, nosyl protecting groups and super-cinnamaldehydes emerge as unexpected and most promising scaffolds to further elaborate on irreversible inhibitors of thiol-mediated uptake and beyond.

Acknowledgements

We thank the NMR and MS platforms for service, and the University of Geneva, including an Innogap Grant (S.M.), the Swiss National Centre of Competence in Research (NCCR) Chemical Biology (J.W., S.M.), the NCCR Molecular Systems Engineering (S.M.), the Swiss NSF (200020 182798 (J.W.), 200020 175486 (S.M.)) and the European Research Council (ERC Consolidator Grant SeleCHEM No. 771170, J.W.) for financial support.

Author Contributions Statement

B. L., *Y. C.* and *D. M.* performed the inhibitor screening, *T. K.*, *A.-T. P.*, *E. L. D.*, *A. K. M.* and *E. G.* synthesized inhibitors, *N. S.*, *J. W.* and *S. M.* directed the study, all authors contributed to experimental design, data interpretation and manuscript writing.

References

[1] Q. Laurent, R. Martinent, B. Lim, A.-T. Pham, T. Kato, J. López-Andarias, N. Sakai, S. Matile, 'Thiol-Mediated Uptake', *JACS Au* **2021**, *1*, 710–728.
[2] A. Tirla, P. Rivera-Fuentes, 'Peptide Targeting of an Intracellular Receptor of the Secretory Pathway', *Biochemistry* **2019**, *58*, 1184–1187.
[3] A. F. L. Schneider, M. Kithil, M. C. Cardoso, M. Lehmann, C. P. R. Hackenberger, 'Cellular uptake of large biomolecules enabled by cell-surface-reactive cell-penetrating peptide additives', *Nat. Chem.* **2021**, *13*, 530–539.
[4] S. Du, S. S. Liew, L. Li, S. Q. Yao, 'Bypassing Endocytosis: Direct Cytosolic Delivery of Proteins', *J. Am. Chem. Soc.* **2018**, *140*, 15986–15996.
[5] A. G. Torres, M. J. Gait, 'Exploiting cell surface thiols to enhance cellular uptake', *Trends Biotechnol.* **2012**, *30*, 185–190.
[6] S. Ulrich, 'Growing Prospects of Dynamic Covalent Chemistry in Delivery Applications', *Acc. Chem. Res.* **2019**, *52*, 510–519.
[7] J. Zhou, Z. Shao, J. Liu, Q. Duan, X. Wang, J. Li, H. Yang, 'From Endocytosis to Nonendocytosis: The Emerging Era of Gene Delivery', *ACS Appl. Bio Mater.* **2020**, *3*, 2686–2701.
[8] X. Meng, T. Li, Y. Zhao, C. Wu, 'CXC-Mediated Cellular Uptake of Miniproteins: Forsaking "Arginine Magic"', *ACS Chem. Biol.* **2018**, *13*, 3078–3086.
[9] J. Lu, H. Wang, Z. Tian, Y. Hou, H. Lu, 'Cryopolymerization of 1,2-Dithiolanes for the Facile and Reversible Grafting-from Synthesis of Protein-Polydisulfide Conjugates', *J. Am. Chem. Soc.* **2020**, *142*, 1217–1221.
[10] J. Zhou, L. Sun, L. Wang, Y. Liu, J. Li, J. Li, J. Li, H. Yang, 'Self-Assembled and Size-Controllable Oligonucleotide Nanospheres for Effective Antisense Gene Delivery through an Endocytosis-Independent Pathway', *Angew. Chem. Int. Ed.* **2019**, *58*, 5236–5240.
[11] D. Oupický, J. Li, 'Bioreducible Polycations in Nucleic Acid Delivery: Past, Present, and Future Trends', *Macromol. Biosci.* **2014**, *14*, 908–922.
[12] Z. Shu, I. Tanaka, A. Ota, D. Fushihara, N. Abe, S. Kawaguchi, K. Nakamoto, F. Tomoike, S. Tada, Y. Ito, Y. Kimura, H. Abe, 'Disulfide-Unit Conjugation Enables Ultrafast Cytosolic Internalization of Antisense DNA and siRNA', *Angew. Chem. Int. Ed.* **2019**, *58*, 6611–6615.

[13] A. Kohata, P. K. Hashim, K. Okuro, T. Aida, 'Transferrin-Appended Nanocaplet for Transcellular siRNA Delivery into Deep Tissues', *J. Am. Chem. Soc.* **2019**, *141*, 2862–2866.
[14] Q. Laurent, N. Sakai, S. Matile, 'The Opening of 1,2-Dithiolanes and 1,2-Diselenolanes: Regioselectivity, Rearrangements, and Consequences for Poly(disulfide)s, Cellular Uptake and Pyruvate Dehydrogenase Complexes', *Helv. Chim. Acta* **2019**, *102*, e1800209.
[15] H. J.-P. Ryser, R. Flückiger, 'Keynote review: Progress in targeting HIV-1 entry', *Drug Discovery Today* **2005**, *10*, 1085–1094.
[16] G. Gasparini, G. Sargsyan, E.-K. Bang, N. Sakai, S. Matile, 'Ring Tension Applied to Thiol-Mediated Cellular Uptake', *Angew. Chem. Int. Ed.* **2015**, *54*, 7328–7331.
[17] Y. Okamoto, R. Kojima, F. Schwizer, E. Bartolami, T. Heinisch, S. Matile, M. Fussenegger, T. R. Ward, 'A cell-penetrating artificial metalloenzyme regulates a gene switch in a designer mammalian cell', *Nat. Commun.* **2018**, *9*, 1943.
[18] E. Derivery, E. Bartolami, S. Matile, M. Gonzalez-Gaitan, 'Efficient Delivery of Quantum Dots into the Cytosol of Cells Using Cell-Penetrating Poly(disulfide)s', *J. Am. Chem. Soc.* **2017**, *139*, 10172–10175.
[19] N. Chuard, G. Gasparini, D. Moreau, S. Lörcher, C. Palivan, W. Meier, N. Sakai, S. Matile, 'Strain-Promoted Thiol-Mediated Cellular Uptake of Giant Substrates: Liposomes and Polymersomes', *Angew. Chem. Int. Ed.* **2017**, *56*, 2947–2950.
[20] Y. Cheng, A.-T. Pham, T. Kato, B. Lim, D. Moreau, J. López-Andarias, L. Zong, N. Sakai, S. Matile, 'Inhibitors of thiol-mediated uptake', *Chem. Sci.* **2021**, *12*, 626–631.
[21] K. Sargsyan, C.-C. Lin, T. Chen, C. Grauffel, Y.-P. Chen, W.-Z. Yang, H. S. Yuan, C. Lim, 'Multi-targeting of functional cysteines in multiple conserved SARS-CoV-2 domains by clinically safe Zn-ejectors', *Chem. Sci.* **2020**, *11*, 9904–9909.
[22] Z. Jin, X. Du, Y. Xu, Y. Deng, M. Liu, Y. Zhao, B. Zhang, X. Li, L. Zhang, C. Peng, Y. Duan, J. Yu, L. Wang, K. Yang, F. Liu, R. Jiang, X. Yang, T. You, X. Liu, X. Yang, F. Bai, H. Liu, X. Liu, L. W. Guddat, W. Xu, G. Xiao, C. Qin, Z. Shi, H. Jiang, Z. Rao, H. Yang, 'Structure of M^{pro} from SARS-CoV-2 and discovery of its inhibitors', *Nature* **2020**, *582*, 289–293.
[23] D. Abegg, G. Gasparini, D. G. Hoch, A. Shuster, E. Bartolami, S. Matile, A. Adibekian, 'Strained Cyclic Disulfides Enable Cellular Uptake by Reacting with the Transferrin Receptor', *J. Am. Chem. Soc.* **2017**, *139*, 231–238.
[24] X. Tang, M. Yang, Z. Duan, Z. Liao, L. Liu, R. Cheng, M. Fang, G. Wang, H. Liu, J. Xu, P. M. Kamau, Z. Zhang, L. Yang, X. Zhao, X. Peng, R. Lai, 'Transferrin receptor is another receptor for SARS-CoV-2 entry', *bioRxiv* **2020**, doi.org/10.1101/2020.10.23.350348.
[25] R. Frei, J. Waser, 'A Highly Chemoselective and Practical Alkynylation of Thiols', *J. Am. Chem. Soc.* **2013**, *135*, 9620–9623.
[26] R. Frei, M. D. Wodrich, D. P. Hari, P.-A. Borin, C. Chauvier, J. Waser, 'Fast and Highly Chemoselective Alkynylation of Thiols with Hypervalent Iodine Reagents Enabled through a Low Energy Barrier Concerted Mechanism', *J. Am. Chem. Soc.* **2014**, *136*, 16563–16573.
[27] D. Abegg, R. Frei, L. Cerato, D. P. Hari, C. Wang, J. Waser, A. Adibekian, 'Proteome-Wide Profiling of Targets of Cysteine reactive Small Molecules by Using Ethynyl Benziodoxolone Reagents', *Angew. Chem. Int. Ed.* **2015**, *54*, 10852–10857.
[28] R. Tessier, J. Ceballos, N. Guidotti, R. Simonet-Davin, B. Fierz, J. Waser, '"Doubly Orthogonal" Labeling of Peptides and Proteins', *Chem* **2019**, *5*, 2243–2263.
[29] R. Tessier, R. K. Nandi, B. G. Dwyer, D. Abegg, C. Sornay, J. Ceballos, S. Erb, S. Cianférani, A. Wagner, G. Chaubet, A. Adibekian, J. Waser, 'Ethynylation of Cysteine Residues: From Peptides to Proteins in Vitro and in Living Cells', *Angew. Chem. Int. Ed.* **2020**, *59*, 10961–10970.
[30] J. Ceballos, E. Grinhagena, G. Sangouard, C. Heinis, J. Waser, 'Cys-Cys and Cys-Lys Stapling of Unprotected Peptides Enabled by Hypervalent Iodine Reagents', *Angew. Chem. Int. Ed.* **2021**, *60*, 9022–9031.
[31] P. Morelli, X. Martin-Benlloch, R. Tessier, J. Waser, N. Sakai, S. Matile, 'Ethynyl benziodoxolones: functional terminators for cell-penetrating poly(disulfide)s', *Polym. Chem.* **2016**, *7*, 3465–3470.
[32] Y. Li, D. P. Hari, M. V. Vita, J. Waser, 'Cyclic Hypervalent Iodine Reagents for Atom-Transfer Reactions: Beyond Trifluoromethylation', *Angew. Chem. Int. Ed.* **2016**, *55*, 4436–4454.
[33] D. P. Hari, P. Caramenti, J. Waser, 'Cyclic Hypervalent Iodine Reagents: Enabling Tools for Bond Disconnection via Reactivity Umpolung', *Acc. Chem. Res.* **2018**, *51*, 3212–3225.
[34] T. Kan, T. Fukuyama, 'Ns strategies: a highly versatile synthetic method for amines', *Chem. Commun.* **2004**, 353–359.
[35] L. J. Macpherson, A. E. Dubin, M. J. Evans, F. Marr, P. G. Schultz, B. F. Cravatt, A. Patapoutian, 'Noxious compounds activate TRPA1 ion channels through covalent modification of cysteines', *Nature* **2007**, *445*, 541–545.
[36] O. Koniev, G. Leriche, M. Nothisen, J.-S. Remy, J.-M. Strub, C. Schaeffer-Reiss, A. Van Dorsselaer, R. Baati, A. Wagner, 'Selective Irreversible Chemical Tagging of Cysteine with 3-Arylpropiolonitriles', *Bioconjugate Chem.* **2014**, *25*, 202–206.
[37] H. F. Motiwala, Y.-H. Kuo, B. L. Stinger, B. A. Palfey, B. R. Martin, 'Tunable Heteroaromatic Sulfones Enhance in-Cell Cysteine Profiling', *J. Am. Chem. Soc.* **2020**, *142*, 1801–1810.
[38] C. Zambaldo, E. V. Vinogradova, X. Qi, J. Iaconelli, R. M. Suciu, M. Koh, K. Senkane, S. R. Chadwick, B. B. Sanchez, J. S. Chen, A. K. Chatterjee, P. Liu, P. G. Schultz, B. F. Cravatt, M. J. Bollong, '2-Sulfonylpyridines as Tunable, Cysteine-Reactive Electrophiles', *J. Am. Chem. Soc.* **2020**, *142*, 8972–8979.
[39] Y.-C. Ahn, V. K. May, G. C. Bedford, A. A. Tuley, W. Fast, 'Discovery of 4,4′-Dipyridylsulfide Analogs as "Switchable Electrophiles" for Covalent Inhibition', *ACS Chem. Biol.* **2021**, *16*, 264–269.
[40] Q. Liu, Y. Sabnis, Z. Zhao, T. Zhang, S. J. Buhrlage, L. H. Jones, N. S. Gray, 'Developing Irreversible Inhibitors of the Protein Kinase Cysteinome', *Chem. Biol.* **2013**, *20*, 146–159.
[41] F. S. Steven, V. Podrazký, 'Evidence for the Inhibition of Trypsin by Thiols', *Eur. J. Biochem.* **1978**, *83*, 155–161.
[42] M. E. B. Smith, F. F. Schumacher, C. P. Ryan, L. M. Tedaldi, D. Papaioannou, G. Waksman, S. Caddick, J. R. Baker, 'Protein Modification, Bioconjugation, and Disulfide Bridging Using

Bromomaleimides', *J. Am. Chem. Soc.* **2010**, *132*, 1960–1965.
[43] A. J. Rojas, C. Zhang, E. V. Vinogradova, N. H. Buchwald, J. Reilly, B. L. Pentelute, S. L. Buchwald, 'Divergent unprotected peptide macrocyclisation by palladium-mediated cysteine arylation', *Chem. Sci.* **2017**, *8*, 4257–4263.
[44] K. Tokunaga, M. Sato, K. Kuwata, C. Miura, H. Fuchida, N. Matsunaga, S. Koyanagi, S. Ohdo, N. Shindo, A. Ojida, 'Bicyclobutane Carboxylic Amide as a Cysteine-Directed Strained Electrophile for Selective Targeting of Proteins', *J. Am. Chem. Soc.* **2020**, *142*, 18522–18531.
[45] A.-T. Pham, S. Matile, 'Peptide Stapling with Anion-π Catalysts', *Chem. Asian J.* **2020**, *15*, 1562–1566.
[46] L. Zong, E. Bartolami, D. Abegg, A. Adibekian, N. Sakai, S. Matile, 'Epidithiodiketopiperazines: Strain-Promoted Thiol-Mediated Cellular Uptake at the Highest Tension', *ACS Cent. Sci.* **2017**, *3*, 449–453.
[47] R. Martinent, J. López-Andarias, D. Moreau, Y. Cheng, N. Sakai, S. Matile, 'Automated high-content imaging for cellular uptake, from the Schmuck cation to the latest cyclic oligochalcogenides', *Beilstein J. Org. Chem.* **2020**, *16*, 2007–2016.
[48] E. Le Du, T. Duhail, M. D. Wodrich, R. Scopelliti, F. Fadaei-Tirani, E. Anselmi, E. Magnier, J. Waser, 'Structure and Reactivity of *N*-Heterocyclic Alkynyl Hypervalent Iodine Reagents', *Chem. Eur. J.* **2021**, doi.org/10.1002/chem.202101475.
[49] G. Cavallo, P. Metrangolo, R. Milani, T. Pilati, A. Priimagi, G. Resnati, G. Terraneo, 'The Halogen Bond', *Chem. Rev.* **2016**, *116*, 2478–2601.
[50] M. S. Taylor, 'Anion recognition based on halogen, chalcogen, pnictogen and tetrel bonding', *Coord. Chem. Rev.* **2020**, *413*, 213270.
[51] L. E. Bickerton, A. J. Sterling, P. D. Beer, F. Duarte, M. J. Langton, 'Transmembrane anion transport mediated by halogen bonding and hydrogen bonding triazole anionophores', *Chem. Sci.* **2020**, *11*, 4722–4729.
[52] R. L. Sutar, S. M. Huber, 'Catalysis of Organic Reactions through Halogen Bonding', *ACS Catal.* **2019**, *9*, 9622–9639.
[53] K. Strakova, L. Assies, A. Goujon, F. Piazzolla, H. V. Humeniuk, S. Matile, 'Dithienothiophenes at Work: Access to Mechanosensitive Fluorescent Probes, Chalcogen-Bonding Catalysis, and Beyond', *Chem. Rev.* **2019**, *119*, 10977–11005.
[54] A. Gini, M. Paraja, B. Galmés, C. Besnard, A. I. Poblador-Bahamonde, N. Sakai, A. Frontera, S. Matile, 'Pnictogen-bonding catalysis: brevetoxin-type polyether cyclizations', *Chem. Sci.* **2020**, *11*, 7086–7091.
[55] J. García-Calvo, J. Maillard, I. Fureraj, K. Strakova, A. Colom, V. Mercier, A. Roux, E. Vauthey, N. Sakai, A. Fürstenberg, S. Matile, 'Fluorescent Membrane Tension Probes for Super-Resolution Microscopy: Combining Mechanosensitive Cascade Switching with Dynamic-Covalent Ketone Chemistry', *J. Am. Chem. Soc.* **2020**, *142*, 12034–12038.
[56] N. Declas, G. Pisella, J. Waser, 'Vinylbenziodoxol(on)es: Synthetic Methods and Applications', *Helv. Chim. Acta* **2020**, *103*, e2000191.
[57] A. K. Mishra, R. Tessier, D. P. Hari, J. Waser, 'Amphiphilic Iodine(III) Reagents for the Lipophilization of Peptides in Water', *Angew. Chem. Int. Ed.* **2021**, doi.org/10.1002/anie.202106458.
[58] D. M. Bautista, P. Movahed, A. Hinman, H. E. Axelsson, O. Sterner, E. D. Högestätt, D. Julius, S.-E. Jordt, P. M. Zygmunt, 'Pungent products from garlic activate the sensory ion channel TRPA1', *Proc. Natl. Acad. Sci. USA* **2005**, *102*, 12248–12252.
[59] J. Sun, Y.-J. Xie, C.-G. Yan, 'Construction of Dispirocyclopentanebisoxindoles via Self-Domino Michael-Aldol Reactions of 3-Phenacylideneoxindoles', *J. Org. Chem.* **2013**, *78*, 8354–8365.

Received June 1, 2021
Accepted June 23, 2021

